Causality and Waveguide Circuit Theory

Dylan F. Williams, *Senior Member, IEEE,* and Bradley K. Alpert

***Abstract*—We develop a new causal power-normalized waveguide equivalent-circuit theory that, unlike its predecessors, results in network parameters usable in both the frequency and time domains in a broad class of waveguides. Enforcing simultaneity of the voltages, currents, and fields and a power normalization fixes all of the parameters of the new theory within a single normalization factor, including both the magnitude and phase of the characteristic impedance of the waveguide. Enforcing simultaneity also ensures that the theory's voltages and currents do not start before their excitation, and that the network parameters of passive devices are causal, a necessary condition for stable time-domain simulations.**

***Index Terms*—Causality, characteristic impedance, microwave-circuit theory, minimum phase.**

I. Introduction

We will develop a new causal power-normalized waveguide circuit theory. We will present an explicit construction algorithm that enforces simultaneity of its voltages and currents with the electric and magnetic fields in the circuit without the TEM, TE, and TM restrictions of classical waveguide circuit theories. This simultaneity will ensure, among other things, that the theory's voltages and currents do not start before their excitation, that the characteristic impedance is always minimum phase, and that the network parameters of passive devices are causal—a necessary condition for stable time-domain simulations.

We will also employ the power normalization of [1] so that the actual time-averaged complex power p in the circuit is equal to $1/2vi^*$, and the actual power crossing a reference plane in the waveguide is equal to the real part of $1/2vi^*$.[1] The simultaneity and power constraints will fix all of the parameters of this new causal circuit theory, including the characteristic impedance Z_0, within a single positive frequency-independent multiplier that defines the overall impedance normalization. We will show explicitly that if the voltages and currents of some other circuit theory are linearly related to the electric and magnetic fields and those voltages and currents are not equal to those of this theory, then they either violate causality or are not power normalized.

Waveguide equivalent-circuit theories prescribe methods for constructing a waveguide voltage v and current i from the electromagnetic fields in uniform waveguides. The intent is to construct v and i so that the electromagnetic problem reduces to a simpler circuit problem that can be solved with conventional circuit simulators.

Classical waveguide equivalent-circuit theories, of which [2] is representative, are based on frequency-independent modal solutions with a constant wave impedance. While we will see that the network parameters of these classic theories satisfy the causality and power-normalization conditions we develop here, they are strictly limited to TEM, TE, and TM waveguides.

The theories of [1] and [3] attempt to eliminate the restriction to TEM, TE, and TM waveguides by adding a power normalization, an approach first suggested by Brews [4]. The power normalizations used in these theories ensure that passive circuits cannot create more power than they absorb, a basic requirement for stable circuit simulation. The normalization ensures, for example, that the real part of the impedance of a passive one-port circuit is always positive.

Nevertheless the waveguide circuit theories of [1] and [3] do not fix all of their parameters uniquely: they additionally require a user-defined integration path to define either the voltage or current. Since they construct v and i independently at each frequency, they also do not explicitly relate the behavior of their parameters in the frequency domain to their behavior in the time domain and, thus, leave unspecified the temporal properties of v and i.

Leaving the temporal properties of v and i unspecified can have serious consequences. For example, the network parameters of passive devices in the circuit theories of [1] and [3] are not constrained to be causal. That is, passive circuits may appear to respond to inputs *before*, rather than after, the input signal reaches the device. This behavior complicates the interpretation of the circuits network parameters in the time domain, and renders them unsuitable for use with conventional time-based simulation tools.

In what follows, we develop a causal power-normalized waveguide equivalent-circuit theory. The theory determines voltages, currents, and network parameters suitable for use in both frequency- and time-domain circuit simulations from the fields of a single-moded waveguide. The theory maintains the simultaneity of the voltages, currents, and fields inherent in classical waveguide circuit theory, but is not restricted to TEM, TE, and TM guides.

II. Voltage and Current

We begin with a closed waveguide that is uniform in the axial direction. The waveguide must have only a single dominant mode and be long enough to support only that mode at a reference plane where v and i are defined. We also require that the dominant mode be unique and distinct from any other modes in the system: modes with degeneracies or modes that bifurcate violate this restriction.

Manuscript received December 1998; revised October 18, 2000.

The authors are with the National Institute of Standards and Technology, Boulder, CO 80303 USA (e-mail: dylan@boulder.nist.gov).

Publisher Item Identifier S 0018-9480(01)02438-3.

[1]The factor of 1/2 appears in the relation for time-averaged power because the complex magnitude of voltages, currents, and fields are defined here as the peak values. The factor of 1/2 does not appear in [1] because there complex magnitudes are defined in terms of the root mean square of the peak values.

We begin with a forward-propagating solution of Maxwell's equation, whose transverse electric- and magnetic-field solutions we can write as $\boldsymbol{e}_{\rm t}(\omega, \boldsymbol{r})e^{-\gamma z}$ and $\boldsymbol{h}_{\rm t}(\omega, \boldsymbol{r})e^{-\gamma z}$, and whose longitudinal electric- and magnetic-field solutions we can write as $e_{\rm z}(\omega, \boldsymbol{r})e^{-\gamma z}$ and $h_{\rm z}(\omega, \boldsymbol{r})e^{-\gamma z}$, where ω is the angular frequency, γ is the propagation constant of the forward mode, $\boldsymbol{r} = (x, y)$ is the transverse coordinate in the guide, and z is the longitudinal position along the guide.

The fields $\boldsymbol{e}_{\rm t}$, $-\boldsymbol{h}_{\rm t}$, $-e_{\rm z}$, and $h_{\rm z}$ with propagation constant $-\gamma$ will also satisfy Maxwell's equations in the guide, and we will call this field solution the backward mode of propagation. To distinguish between the forward and backward modes of propagation, we use the convention of [1]. That is, we insist that, in lossy guides, the real part of the complex power

$$p_0(\omega) \equiv \int \boldsymbol{e}_{\rm t}(\omega, \boldsymbol{r}) \times \boldsymbol{h}_{\rm t}^*(\omega, \boldsymbol{r}) \cdot \boldsymbol{z}\, d\boldsymbol{r} \tag{1}$$

carried in the $+z$-direction by the forward mode is positive. If $\mathrm{Re}(p_0) = 0$, as occurs in an evanescent waveguide mode, we use the condition $\mathrm{Re}(\gamma) > 0$, which forces the mode to decay with z. This convention uniquely identifies the forward and backward modes, and resolves any phase ambiguities in the modal fields, γ, and p_0.

We introduce the voltage $v(\omega, z)$ and frequency-dependent normalization $v_0(\omega)$ with

$$\begin{aligned}\boldsymbol{E}_{\rm t}(\omega, \boldsymbol{r}, z) &= \left[c_+(\omega)e^{-\gamma z} + c_-(\omega)e^{\gamma z}\right]\boldsymbol{e}_{\rm t}(\omega, \boldsymbol{r}) \\ &\equiv \frac{v(\omega, z)}{v_0(\omega)}\,\boldsymbol{e}_{\rm t}(\omega, \boldsymbol{r})\end{aligned} \tag{2}$$

and the current $i(\omega, z)$ and normalization $i_0(\omega)$ with

$$\begin{aligned}\boldsymbol{H}_t(\omega, \boldsymbol{r}, z) &= \left[c_+(\omega)e^{-\gamma z} - c_-(\omega)e^{\gamma z}\right]\boldsymbol{h}_{\rm t}(\omega, \boldsymbol{r}) \\ &\equiv \frac{i(\omega, z)}{i_0(\omega)}\,\boldsymbol{h}_{\rm t}(\omega, \boldsymbol{r})\end{aligned} \tag{3}$$

where c_+ and c_- are the amplitudes of the mode in the forward and backward directions. The two normalizing factors v_0 and i_0 define v and i in terms of the modal field solution $\{\boldsymbol{e}_{\rm t}, \boldsymbol{h}_{\rm t}\}$, which has a fixed, but unspecified, normalization.

We write the total transverse electric field $\hat{\boldsymbol{E}}_{\rm t}(t, \boldsymbol{r}, z)$ and magnetic field $\hat{\boldsymbol{H}}_{\rm t}(t, \boldsymbol{r}, z)$ at a given time t in terms of their frequency-domain representations as

$$\hat{\boldsymbol{E}}_{\rm t}(t, \boldsymbol{r}, z) = \frac{1}{2\pi}\int_{-\infty}^{\infty} \boldsymbol{E}_{\rm t}(\omega, \boldsymbol{r}, z)e^{j\omega t}\, d\omega \tag{4}$$

and

$$\hat{\boldsymbol{H}}_{\rm t}(t, \boldsymbol{r}, z) = \frac{1}{2\pi}\int_{-\infty}^{\infty} \boldsymbol{H}_{\rm t}(\omega, \boldsymbol{r}, z)e^{j\omega t}\, d\omega. \tag{5}$$

We define the normalized transverse modes $\{\boldsymbol{e}'_{\rm t}, \boldsymbol{h}'_{\rm t}\}$ to be

$$\boldsymbol{e}'_{\rm t}(\omega, \boldsymbol{r}) \equiv \frac{\boldsymbol{e}_{\rm t}(\omega, \boldsymbol{r})}{v_0(\omega)} \quad \boldsymbol{h}'_{\rm t}(\omega, \boldsymbol{r}) \equiv \frac{\boldsymbol{h}_{\rm t}(\omega, \boldsymbol{r})}{i_0(\omega)} \tag{6}$$

which imply $\boldsymbol{E}_{\rm t} = v\boldsymbol{e}'_{\rm t}$ and $\boldsymbol{H}_{\rm t} = i\boldsymbol{h}'_{\rm t}$. The power normalization is achieved with the constraint

$$v_0(\omega)i_0^*(\omega) = p_0(\omega) \equiv \int \boldsymbol{e}_{\rm t}(\omega, \boldsymbol{r}) \times \boldsymbol{h}_{\rm t}{}^*(\omega, \boldsymbol{r}) \cdot \boldsymbol{z}\, d\boldsymbol{r} \tag{7}$$

where the integral in (7) is over the entire guide cross section. This normalization implies that $\int \boldsymbol{e}'_{\rm t}(\omega, \boldsymbol{r}) \times \boldsymbol{h}'^*_{\rm t}(\omega, \boldsymbol{r}) \cdot \boldsymbol{z}\, d\boldsymbol{r} = 1$, and ensures that the total time-averaged complex power p is given by $p \equiv 1/2 \int \boldsymbol{E}_{\rm t}(\omega, \boldsymbol{r}) \times \boldsymbol{H}^*_{\rm t}(\omega, \boldsymbol{r}) \cdot \boldsymbol{z}\, d\boldsymbol{r} = 1/2vi^*$, and that the actual power transmitted across a reference plane is given by the real part of p.

Equations (4)–(6) imply that

$$\begin{aligned}\hat{\boldsymbol{E}}_{\rm t}(t, \boldsymbol{r}, z) &\equiv \hat{v}(t, z) \circledast \hat{\boldsymbol{e}}'_{\rm t}(t, \boldsymbol{r}) \\ \hat{\boldsymbol{H}}_{\rm t}(t, \boldsymbol{r}, z) &\equiv \hat{i}(t, z) \circledast \hat{\boldsymbol{h}}'_{\rm t}(t, \boldsymbol{r})\end{aligned} \tag{8}$$

where Fourier transformation gives the temporal voltage

$$\hat{v}(t, z) \equiv \frac{1}{2\pi}\int_{-\infty}^{\infty} v(\omega, z)e^{j\omega t}\, d\omega \tag{9}$$

and the temporal current

$$\hat{i}(t, z) \equiv \frac{1}{2\pi}\int_{-\infty}^{\infty} i(\omega, z)e^{j\omega t}\, d\omega \tag{10}$$

and $\circledast$ represents convolution with respect to the time t.

We say that a function $\hat{\boldsymbol{F}}(t, \boldsymbol{r})$ starts at a time t_0 if $\hat{\boldsymbol{F}}(t, \boldsymbol{r}) = 0$ for $t < t_0$ and is nonvanishing at some $\boldsymbol{r}$ starting at $t = t_0$. We observe that if $\hat{\boldsymbol{e}}'_{\rm t}$ and $\hat{\boldsymbol{h}}'_{\rm t}$ were to start at $t = 0$, then the temporal voltage $\hat{v}$ would start simultaneously with $\hat{\boldsymbol{E}}_{\rm t}$, and the temporal current $\hat{i}$ would start simultaneously with $\hat{\boldsymbol{H}}_{\rm t}$.

In what follows, we will present a prescription for determining v_0 and i_0 in a single-mode waveguide that is consistent with the power normalization (7) *and* such that $\hat{\boldsymbol{e}}'_{\rm t}$ and $\hat{\boldsymbol{h}}'_{\rm t}$ do, in fact, start at $t = 0$. This prescription will, therefore, ensure $p = vi^*$ *and* simultaneity $\hat{v}$ of and $\hat{\boldsymbol{E}}_{\rm t}$ and of $\hat{i}$ and $\hat{\boldsymbol{H}}_{\rm t}$.

III. TEM, TE, AND TM GUIDES

Construction of causal v_0 and i_0 that satisfy the power normalization (7) is straightforward in TEM, TE, and TM guides. In those guides, there exists a unique wave impedance $Z_{\rm w}(\omega)$ and the modal fields can be written as

$$\boldsymbol{e}_{\rm t}(\omega, \boldsymbol{r}) = \boldsymbol{f}(\boldsymbol{r}) \quad \boldsymbol{h}_{\rm t}(\omega, \boldsymbol{r}) = \frac{\boldsymbol{z} \times \boldsymbol{f}(\boldsymbol{r})}{Z_{\rm w}(\omega)} \tag{11}$$

where $\boldsymbol{f}(\boldsymbol{r})$ is real. Without loss of generality, we can set $\int |\boldsymbol{f}(\boldsymbol{r})|^2\, d\boldsymbol{r} = 1$.

Appendix C uses the temporal form of Maxwell's equations to show that the temporal wave impedance $\hat{Z}_{\rm w}(t)$ and temporal wave admittance $\hat{Y}_{\rm w}(t)$ must equal zero for $t < 0$. Since $Z_{\rm w}(\omega)$ may have zeros or singularities on the real axis, we must take care when choosing any branch cuts to ensure that the Fourier transform of $Z_{\rm w}(\omega)$ has these same temporal properties. That is, we must choose any branch cuts to be in the upper half of the ω plane so that $Z_{\rm w}(\omega)$ will be analytic in the lower half of the ω plane.

With this normalization, $p_0 = 1/Z_{\rm w}^*$, $v_0 = \lambda$, and $i_0 = 1/(\lambda Z_{\rm w})$, where λ is a positive constant multiplier, satisfy the

power normalization (7). We also have $\hat{\boldsymbol{e}}'(t, \boldsymbol{r}) = \lambda^{-1}\delta(t)\boldsymbol{f}(\boldsymbol{r})$ and $\hat{\boldsymbol{h}}'(t, \boldsymbol{r}) = \lambda\delta(t)\boldsymbol{z} \times \boldsymbol{f}(\boldsymbol{r})$, where δ is the Dirac delta function, so we see that $\hat{v}$ starts simultaneously with $\hat{\boldsymbol{E}}_{\mathrm{t}}$, and $\hat{i}$ starts simultaneously with $\hat{\boldsymbol{H}}_{\mathrm{t}}$.

If we choose $\lambda = 1$, then $\boldsymbol{E}_{\mathrm{t}} = v\boldsymbol{e}_{\mathrm{t}}$ and $\boldsymbol{H}_{\mathrm{t}} = iZ_{\mathrm{w}}\boldsymbol{h}_{\mathrm{t}} = i\boldsymbol{z} \times \boldsymbol{e}_{\mathrm{t}}$, and we see that v and i correspond to the voltages and currents of the classic theory. Thus, in both the classic waveguide circuit theory *and* our causal generalization of that theory, the voltage and current start simultaneously with the electric and magnetic fields, and the characteristic impedance Z_0 is proportional to the wave impedance of TEM, TM, and TE modes. Other choices, such as setting $|Z_0| = 1$ in lossless rectangular waveguide, which is allowed in [1], [3], and [5], will not be consistent with the classic waveguide circuit theory or with our causal generalization.

IV. Non-TEM, Non-TE, and Non-TM Guides

Appendix A constructs a normalizing voltage v_0' such that the time-domain voltage $\hat{v}'$ associated with it and the electric field start at the same time when the modal electric field $\boldsymbol{e}_{\mathrm{t}}$ is separable and can be expanded as a finite sum

$$\boldsymbol{e}_{\mathrm{t}}(\omega, \boldsymbol{r}) = \sum_{m=1}^{n} c_m(\omega)\boldsymbol{f}_m(\boldsymbol{r}) \tag{12}$$

where the $c_m(\omega)$ are rational functions of ω and the $\boldsymbol{f}_m(\boldsymbol{r})$ are real vector functions that satisfy the orthogonality condition

$$\int \boldsymbol{f}_m(\boldsymbol{r}) \cdot \boldsymbol{f}_j(\boldsymbol{r})\, d\boldsymbol{r} \equiv \begin{cases} 1, & \text{if } m = j \\ 0, & \text{if } m \neq j. \end{cases} \tag{13}$$

In the following section, we will argue that this form is not overly restrictive.

A similar argument shows that when $\boldsymbol{h}_{\mathrm{t}}$ separates in this way, we can construct a normalizing current i_0' such that the time-domain current $\hat{i}'$ associated with it and the magnetic field start at the same time.

We now apply a Wiener–Hopf decomposition [6] to the function $g \equiv p_0/v_0'i_0'^*$. Define the auxiliary function G from $\arg(G) = \arg(g)$ and $\mathcal{H}(\ln|G|) = \arg(g)$, where $\mathcal{H}$ is the Hilbert transform (see Appendix II for a discussion of minimum-phase functions and the Hilbert transform $\mathcal{H}$). We then have $\mathcal{H}(\ln|G|) = \arg(G) = \arg(g)$, with G being the minimum phase by construction.

Then define K_{v} and K_{i} from $\ln|K_{\mathrm{v}}| \equiv 1/2(\ln|g| + \ln|G|)$, $\ln|K_{\mathrm{i}}| \equiv 1/2(\ln|g| - \ln|G|)$, $\arg(K_{\mathrm{v}}) \equiv \mathcal{H}(\ln|K_{\mathrm{v}}|)$, and $\arg(K_{\mathrm{i}}) \equiv \mathcal{H}(\ln|K_{\mathrm{i}}|)$. These conditions imply that $|K_{\mathrm{v}}| = \sqrt{|gG|}$ and $|K_{\mathrm{i}}| = \sqrt{|g/G|}$. Finally, define v_0 and i_0 from $v_0 \equiv \lambda K_{\mathrm{v}}v_0'$ and $i_0 \equiv K_{\mathrm{i}}i_0'/\lambda$, where λ is a positive constant multiplier.

K_{v} and K_{i} are minimum phase by construction, thus, $\hat{v}$ starts simultaneously with $\hat{v}'$ and, therefore, with $\hat{\boldsymbol{E}}_{\mathrm{t}}$, and $\hat{i}'$ starts simultaneously with $\hat{i}'$ and, therefore, with $\hat{\boldsymbol{H}}_{\mathrm{t}}$. Furthermore, $v_0i_0^* = K_{\mathrm{v}}K_{\mathrm{i}}^*p_0/g$, $|v_0i_0^*| = |p_0|$, and $\arg(v_0i_0^*) = \arg(K_{\mathrm{v}}) - \arg(K_{\mathrm{i}}) + \arg(p_0) - \arg(g) = \arg(p_0)$, thus, v_0 and i_0 satisfy the power normalization constraint (7). Thus, the voltages and currents are both causal and power normalized.

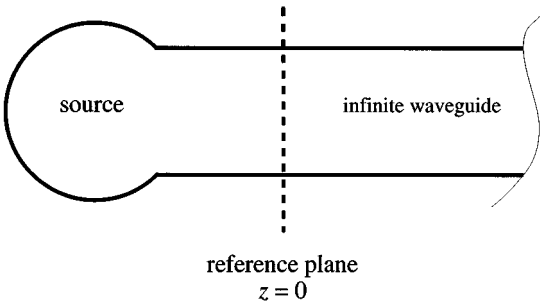

Fig. 1. Source connected to an infinite waveguide.

V. Limitations

For TEM, TM, and TE modes, our causal theory reduces to the classic circuit theory. These modes include a number of useful idealizations for which explicit expressions for the modal fields and wave impedance are available. In treating these modes, we have placed no restriction on the form of the wave impedance Z_{w}: it need not have a rational approximation.

We used the construction algorithm of Appendix A to overcome the TEM, TE, and TM restriction of the classic circuit theory. That algorithm requires that the c_m in (12) be rational functions of ω. Nevertheless, the form of (12) is general enough to represent any piecewise continuous modal field up to any finite frequency to any desired accuracy. This is because rational functions are sufficient to approximate to arbitrary precision any function analytic in a half-plane and either regular at infinity or possessing an isolated pole there [6]. Thus, we can approximate the wave solutions in guides constructed entirely of materials with finite loss as accurately as we wish with this expansion, and we see that it is not overly restrictive in practice. However, we may not be able to treat some lossless idealizations that are neither TEM, TM, nor TE with the two approaches suggested here.

VI. Characteristic Impedance

Fig. 1 shows a source connected to an infinite waveguide with the reference plane chosen far enough away from the source to satisfy the single-mode restrictions of this theory. Since only the forward mode is present in the situation illustrated in Fig. 1, we have, for this special case, $c_- = 0$

$$\begin{aligned} v_+(\omega, z) &= v_0(\omega)c_+(\omega)e^{-\gamma z} \\ i_+(\omega, z) &= i_0(\omega)c_+(\omega)e^{-\gamma z} \end{aligned} \tag{14}$$

thus,

$$Z_0(\omega) \equiv \left.\frac{v(\omega, z)}{i(\omega, z)}\right|_{c_-=0} = \frac{v_0(\omega)}{i_0(\omega)} \tag{15}$$

which is indeed independent of z. Thus,

$$\begin{aligned} \arg(Z_0(\omega)) &\equiv \arg\left(\frac{v_0(\omega)}{i_0(\omega)}\right) \\ &= \arg\left(v_0(\omega)i_0^*(\omega)\right) \\ &\equiv \arg\left(p_0(\omega)\right) \end{aligned} \tag{16}$$

is fixed by the power normalization (7) [1].

Maxwell's equations imply that, when only the forward mode is present, $\hat{\boldsymbol{E}}_{\rm t}$ and $\hat{\boldsymbol{H}}_{\rm t}$ arrive simultaneously (see Appendix C), thus, $\hat{v}$ and $\hat{i}$ must as well. Thus, in our causal theory, $Z_0 = v/i$ must be a minimum phase function and

$$\mathcal{H}\Big[\ln\big(|Z_0(\omega)|\big)\Big] = \arg\big[Z_0(\omega)\big]. \tag{17}$$

Once $\arg(Z_0)$ is determined by the power normalization (7) and the magnitude of Z_0 is restricted by (17), the space of solutions for $|Z_0|$ is defined by

$$\big|Z_0(\omega)\big| = \lambda e^{-\mathcal{H}(\arg[Z_0(\omega)])} \tag{18}$$

where λ is a real positive frequency-independent constant that determines the overall impedance normalization.[2] Thus, we see that our causal power-normalized circuit theory fixes the characteristic impedance to within the constant multiplier λ. As a corollary, if the guide has a unique wave impedance, that wave impedance will be minimum phase (see also Appendix C).

VII. Uniqueness

The causal power-normalized voltages and currents are unique. Imagine that there are two possible voltage normalizations v_{01} and v_{02} in the theory. We require that, for any excitation in the guide, the temporal voltage $\hat{v}$ must start simultaneously with the electric field so the two temporal voltages $\hat{v}_1$ and $\hat{v}_2$ associated with v_{01} and v_{02} will always start at the same time as well.

Simultaneous starting times of $\hat{v}_1$ and $\hat{v}_2$ for any excitation implies that $v_1/v_2 = v_{01}/v_{02}$ is minimum phase, thus, $\arg(v_{01}/v_{02}) = \mathcal{H}[\ln(v_{01}/v_{02})]$. However, once we have chosen the constant multiplier λ and, thus, fixed Z_0, we must also have $|v_0|^2 = |v_0(p_0/i_0{}^*)| = |Z_0 p_0|$, which implies that $|v_{01}/v_{02}| = 1$. Thus, $\arg(v_{01}/v_{02}) = 0$ and $v_{01} = v_{02}$. A similar argument shows that i_0 is unique.

We have just shown that the requirement that the voltages and currents be linearly related to and start simultaneously with the electric and magnetic fields and the power normalization imply that the voltages and currents are unique to within a constant multiplier λ. We conclude that if the voltages and currents of some other circuit theory are also linearly related to the electric and magnetic fields and those voltages and currents are not equal to those of this theory for some λ, then they either must violate causality or must not be power normalized.

VIII. Causality Condition

Consider the passive circuit of Fig. 2. It connects an input waveguide with voltages and currents v_1 and i_1 at the reference plane on the left-hand side far enough from the source and circuit to satisfy the single-mode assumption of this theory to an output waveguide with voltages and currents v_2 and i_2 at the reference plane on the right-hand side, again, far enough from the circuit to satisfy our single-mode assumption.

[2]Equation (18) results from two facts: the Hilbert transform has a null space consisting of the constant functions and $\mathcal{H}[\mathcal{H}[f(\omega)]] = -f(\omega) + c$, where c is a real positive frequency-independent constant.

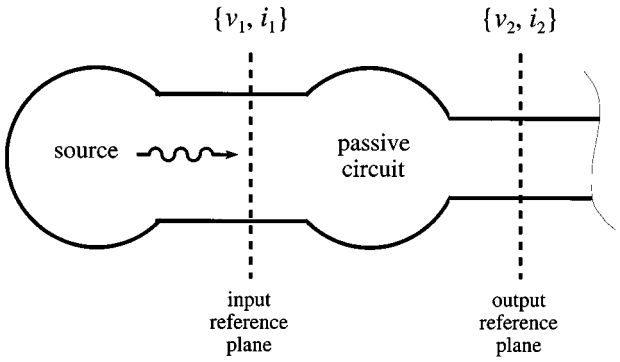

Fig. 2. Source exciting a passive circuit connected to another waveguide.

If the voltage or current at the output were to start before the voltage and current at the input, the fields at the output would have to have started before the fields at the input. This is clearly not possible, thus, we conclude that the voltage at the output always starts after the voltage at the input. This shows that transfer functions such as Z_{21} that determine voltage or current at the output from voltage or current at the input are causal. A similar argument shows that the "driving-point" impedances [7] of the system are minimum phase.

In essence, by enforcing simultaneity in our causal circuit theory, the causal properties of the actual electromagnetic fields in the circuits are preserved by the theory's voltages and currents. This is significant because causal network parameters are a basic requirement for stable time-domain circuit simulation.

IX. Application to the MIS Transmission Line

Metal–insulator–semiconductor (MIS) transmission lines are neither TEM, TE, nor TM. The theories of [1] and [3] suggest combining either a voltage normalization

$$v_0 = -\int_{\rm path} \boldsymbol{e}_{\rm t} \cdot d\boldsymbol{l} \tag{19}$$

or a current normalization

$$i_0 = \oint_{\substack{\rm closed\\ \rm path}} \boldsymbol{h}_{\rm t} \cdot d\boldsymbol{l} \tag{20}$$

with the power constraint of (7) to construct v and i. However, different choices of voltage and current paths in (19) and (20) are possible. Now we will show that not all of these choices are consistent with our causal circuit theory.

We will illustrate the various choices of voltage and current paths with the $\rm TM_{01}$ mode of the infinitely wide MIS line investigated in [8]. This MIS line consists of a 1.0-μm-thick metal signal plane with a conductivity of 3×10^7 S/m separated from the 100-μm-thick 100 $\Omega \cdot$ cm silicon supporting substrate by a 1.0-μm-thick oxide with conductivity of 10^{-3} S/m. The ground conductor on the back of the silicon substrate is infinitely thin and perfectly conducting.

Fig. 3 compares the voltage drop $v_{\rm ox}$ across the oxide layer to the total voltage drop $v_{\rm t}$ across both the oxide and substrate in our MIS line. The figure shows that the ratio of these quantities, which is marked with hollow circles, displays a complicated evolution with frequency. The figure not only illustrates

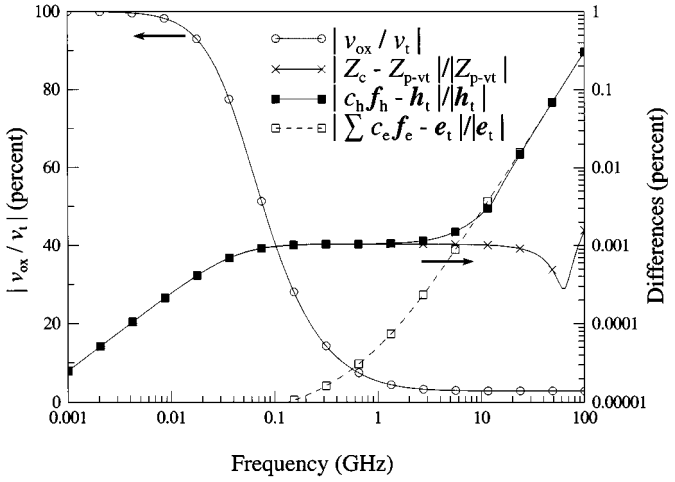

Fig. 3. Ratios of oxide voltage to the total voltage of the MIS line, differences between the approximate fields and exact field solutions, and the difference between the causal characteristic impedance and power/total-voltage characteristic impedances. The ratios are plotted against the left-hand-side axis, while the differences are plotted on the right-hand-side axis. All values are percentages.

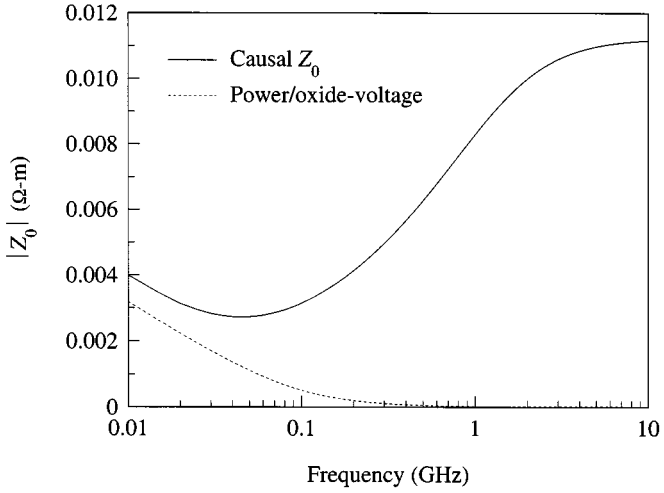

Fig. 4. $|Z_0|$ for the MIS transmission line of [8].

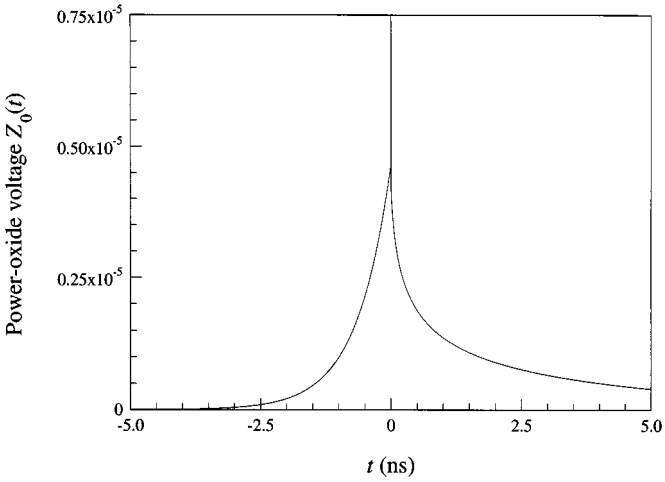

Fig. 5. Fourier transform of the characteristic impedance labeled "Power/oxide-voltage" of Fig. 4.

the complex interaction of the electric field with the dielectrics, but also the large differences between these two voltage definitions in the MIS line.

The conventional circuit theories of [1] and [3] do not specify the voltage path uniquely, and the choice is not obvious. For example, devices embedded in MIS lines are typically fabricated on the silicon surface; they are connected to the signal line with vias through the oxide and to the ground with ohmic contacts at the silicon surface. This suggests that a voltage path $v_{\rm ox}$ in the MIS line from the silicon surface through the oxide to the signal line, not the total voltage v_t, might correspond most closely to the actual voltage seen by the device and be the best normalizing voltage in the circuit theory.

We used the construction procedure of Appendix A to determine the causal power-normalized voltage and current for our MIS line. To construct the voltage, we used two basis functions and multiplying rational functions formed from the ratios of first-order polynomials in ω to approximate the electric field. The first basis function $f_{\rm e1}$ was uniform in the oxide and zero in the substrate, while the second basis function $f_{\rm e2}$ was uniform in the substrate and zero in the oxide. The dashed curve marked with hollow squares plots the maximum value of $|\sum c_{\rm em}\boldsymbol{f}_{em} - \boldsymbol{e}_{\rm t}|/|\boldsymbol{e}_{\rm t}|$ at each frequency point on the right axis. The curve shows that our rational function approximation to the actual fields of the MIS line is extremely accurate.

We expanded the magnetic field using only a single constant basis function in the oxide and substrate. The solid curve marked with solid squares plots the maximum value of error we incurred with this choice of basis function.

When we applied the procedure outlined in Appendix A to these basis functions to construct the causal power-normalized voltage, we found that it equaled the total voltage $v_{\rm t}$ across the line, and that the causal power-normalized current was nearly equal to the current in the signal conductor of the MIS line. The solid line of Fig. 3 marked with crosses plots the difference between the causal power-normalized characteristic impedance $Z_{\rm c}$ we constructed in this way and the power/total-voltage characteristic impedance $Z_{\rm p-v}$, where $Z_{\rm p-v}$ is defined from the power constraint and the total voltage $v_{\rm t}$ across the oxide and substrate. The agreement is excellent.

The solid curve in Fig. 4, which is labeled "Causal Z_0," corresponds to the magnitude of the causal power-normalized characteristic impedance. When we added $Z_{\rm p-v}$ to this figure, the two curves were indistinguishable.

However, Fig. 4 shows that the characteristic impedance defined from the power constraint of (7) and the voltage $v_{\rm ox}$ across the oxide, which is labeled "Power/oxide-voltage," differs significantly from the characteristic impedance required by the causal theory presented here. This shows that using the oxide voltage $v_{\rm ox}$ does, in fact, affect the characteristic impedance greatly, as one might expect from the ratios plotted in Fig. 3.

Fig. 5 shows the Fourier transform of the characteristic impedance defined with the voltage path through the oxide and illustrates the difficulty with this definition of voltage and the resulting characteristic impedance: the guide will respond to input signals before the excitation reaches it.

This example illustrates an important contribution of the causal theory presented here: it replaces the subjective and sometimes misleading "common-sense" criteria for defining Z_0 in guides that are neither TEM, TE, or TM with a clear and unambiguous procedure that guarantees causal responses. This new approach should be especially useful in complex transmission structures where the choice of voltage and current paths is not intuitively obvious.

X. Error in $|Z_0|$

The magnitude of Z_0 in our causal circuit theory may be determined from the phase of p_0 through a Hilbert transform relationship (18). Evaluating the Hilbert transform in (18) requires integrating over all frequencies. Ignorance of the phase of p_0 at frequencies above those at which the theory is to be applied will result in errors in $|Z_0|$ at the frequencies where the theory is applied.

Appendix D develops a bound for the error in $|Z_0|$ at a given frequency ω when the $\arg(p_0)$ is known exactly up to some greater frequency ω_0. The result is

$$\frac{\omega_0^2-\omega^2}{\omega_0^2} \le \left|\frac{Z_0'}{Z_0}\right| \le \frac{\omega_0^2}{\omega_0^2-\omega^2} \tag{21}$$

where Z_0 is the actual characteristic impedance and Z_0' is the value of characteristic impedance we determine from incorrect assumptions about the high frequency behavior of $\arg(p_0)$.

The expression in (21) shows that the error in $|Z_0'|$ can be made as small as required if we are willing to restrict the frequencies ω to which we apply the theory to frequencies much smaller than ω_0, the frequency to which we evaluate the phase of p_0. Although the convergence indicated by (21) is slow, it corresponds to a worst-case scenario: convergence for more forgiving phase errors will be better. However, it should perhaps be emphasized that, while small errors in $|Z_0|$ will sometimes be unavoidable, the resulting characteristic impedance will be causal and have phase equal to $\arg(p_0)$ where the phase of p_0 is known.

XI. Conclusion

We have presented a causal power-normalized waveguide circuit theory that overcomes the TEM, TE, and TM restrictions of classic waveguide circuit theories. The network parameters of the causal circuit theory presented here preserve the causal properties of the actual circuit and the power in the network. This is significant because these properties are required for stable time-domain circuit simulation. Since classical waveguide circuit theories also enforce these properties in TEM, TE, and TM guides, we can say that this theory conserves the essential attributes of the classical waveguide circuit theory in a more general setting.

In the causal circuit theory, the magnitude of the characteristic impedance is related to its temporal properties, not to its properties in the frequency domain. This adds a new perspective to the debate over the relative merits of the various impedance normalizations possible in waveguide equivalent-circuit theories. The implications have been further explored in [9]–[11].

We could have applied causality constraints to an analogous reciprocity-normalized circuit theory [12]. However, the new reciprocity-normalized theory would fail to enforce the passivity condition required for stable circuit simulation. That condition ensures, for example, that the real part of the impedance of a passive one-port circuit is always positive. Our causal power-normalized theory, on the other hand, explicitly enforces the passivity and causality conditions, both of which are needed for stable time-domain simulation.

Appendix A
Construction of v_0

Referring to Fig. 1, we seek a normalizing voltage $v_0'(\omega)$ when $\boldsymbol{e}_{\rm t}$ can be written in the form of (12). We wish to construct the normalizing voltage v_0' so that the temporal voltage $\hat{v}'(t,0)$ will start exactly when the electric field arrives at $z=0$. That is, if $\hat{v}'(t,0)=0$ for $t<0$, then the electric field at $z=0$ vanishes for times $t<0$ and vice versa.

Consider the normalizing voltage

$$v_0'(\omega) \equiv \sum_{m=1}^{n} a_m(\omega) \int \boldsymbol{f}_m(\boldsymbol{r}) \cdot \boldsymbol{e}_{\rm t}(\omega,\boldsymbol{r})\, d\boldsymbol{r} \tag{22}$$

where $a_m(\omega)$ are polynomials in ω. This normalizing voltage is defined so that

$$v_0'(\omega) \equiv \sum_{m=1}^{n} a_m(\omega) c_m(\omega). \tag{23}$$

Referring again to Fig. 1, only the single forward mode is present, thus, the voltage v' associated with the normalizing voltage v_0' at $z=0$ is

$$\begin{aligned} v'(\omega,0) &\equiv c_+(\omega) v_0'(\omega) \\ &= \sum_{m=1}^{n} a_m(\omega) \int \boldsymbol{f}_m(\boldsymbol{r}) \cdot \boldsymbol{E}_{\rm t}(\omega,\boldsymbol{r},0)\, d\boldsymbol{r} \end{aligned} \tag{24}$$

and in the time domain is

$$\hat{v}'(t,0) = \sum_{m=1}^{n} \hat{a}_m(t) \circledast \int \boldsymbol{f}_m(\boldsymbol{r}) \cdot \hat{\boldsymbol{E}}_{\rm t}(t,\boldsymbol{r},0)\, d\boldsymbol{r}. \tag{25}$$

Since the a_m are polynomials, they have no poles at all and are analytic everywhere. As a result, $\hat{a}_m(t)=0$ for $t<0$ (see Appendix B). Thus, if the electric field vanishes for $t<0$, then so do its moments with respect to the $\boldsymbol{f}_m$, and we see that, by construction, a vanishing electric field for $t<0$ implies that $\hat{v}'(t,0)=0$ for $t<0$.

We will now show that it is possible to construct the polynomials a_m so that the inverse is true as well. That is, so that $\hat{v}'(t,0)=0$ for $t<0$ implies that the moments of the electric field with respect to the $\boldsymbol{f}_m$ and, hence, the electric field itself, vanish for $t<0$. In essence, we will show that there are enough degrees of freedom available in the choice of the polynomials a_m that we can eliminate all of the poles in the lower half of the ω plane from an expression that determines the moments of the electric field from v'. This will ensure that the expression is analytic in the lower half-plane and, thus, that their Fourier transforms are zero for $t<0$.

The mth moment of the total electric field with respect to $\boldsymbol{f}_m$ is

$$\begin{aligned}\int \boldsymbol{f}_m(\boldsymbol{r}) \cdot \boldsymbol{E}_t(\omega, \boldsymbol{r}, 0)\, d\boldsymbol{r} &= \frac{v'(\omega, 0)}{v_0'(\omega)} \int \boldsymbol{f}_m(\boldsymbol{r}) \cdot \boldsymbol{e}_t(\omega, \boldsymbol{r})\, d\boldsymbol{r} \\ &= \frac{v'(\omega, 0)}{v_0'(\omega)}\, c_m(\omega) \\ &= I_m^{-1}(\omega) v'(\omega). \end{aligned} \tag{26}$$

If for some m, I_m^{-1} has no poles in the lower half of the ω plane, then $\hat{v}'(t, 0) = 0$ for $t < 0$ implies that the mth moment of the total electric field vanishes for $t < 0$. Our aim is to show that we can pick the a_m so that none of the I_m^{-1} have any poles at all. We will do this by showing that we can construct the a_m so that none of the I_m have zeros.

We can write the c_m as $c_m(\omega) \equiv P_m(\omega)/Q_m(\omega)$, where the P_m and Q_m are polynomials in ω, and expand the I_m as

$$\begin{aligned} I_m(\omega) &\equiv \frac{v_0'(\omega)}{c_m(\omega)} \\ &= \frac{\sum_{j=1}^{n} a_j(\omega) c_j(\omega)}{c_m(\omega)} \\ &= \frac{Q_m(\omega)}{P_m(\omega)} \sum_{j=1}^{n} a_j(\omega) \frac{P_j(\omega)}{Q_j(\omega)}. \end{aligned} \tag{27}$$

We can rearrange (27) to obtain a single common denominator

$$I_m(\omega) = \frac{\sum_j \left(a_j(\omega) P_j(\omega) \prod_{k \neq j} Q_k(\omega) \right)}{P_m(\omega) \prod_{l \neq m} Q_l(\omega)} = \frac{\sum_j a_j(\omega) I_j'(\omega)}{I_m'(\omega)} \tag{28}$$

where

$$I_j'(\omega) \equiv P_j(\omega) \prod_{k \neq j} Q_k(\omega). \tag{29}$$

The numerator of (28) is independent of the index m.

Define $G(\omega)$ to be a greatest common divisor of the I_j'. That is, G is a polynomial of largest possible order such that $I_j' = I_j'' G$, where $I_j''(\omega)$ is a polynomial of order less than or equal to the order of I_j'. The Euclidian algorithm provides a procedure for finding a set of a_j so that $\sum a_j(\omega) I_j'(\omega) = G(\omega)$ [13]. Thus, we can write (28) as

$$I_m(\omega) = \frac{\sum_j a_j(\omega) I_j'(\omega)}{I_m'(\omega)} = \frac{G(\omega)}{I_m'(\omega)} = \frac{1}{I_m''(\omega)}. \tag{30}$$

We have just shown that it is possible to construct a_m so that the I_m in (26) have no zeroes. This guarantees that we can construct a normalizing voltage v_0' from the modal fields such that the voltage v' associated with it is zero for times $t < 0$ whenever the electric field is zero for $t < 0$ and vice versa. That is, we have constructed a voltage $\hat{v}'(t, 0)$ that starts simultaneously with the electric field.

Appendix B
Minimum Phase Functions

Throughout this paper, we denote the frequency-domain representation of a function as $F(\omega)$, and its time-domain representation as $\hat{F}(t)$, where ω is the angular frequency and t is the time. Here, $\hat{F}(t)$ is the inverse Fourier transform of $F(\omega)$

$$\hat{F}(t) \equiv \frac{1}{2\pi} \int_{-\infty}^{\infty} F(\omega) e^{j\omega t}\, d\omega \tag{31}$$

where t is real, and the integration in (31) is performed over real values of ω. If $F(\omega)$ has poles on the real ω axis, we use the limiting value of the integral in (31) as the integration contour approaches the real axis from below. $F(\omega)$ is the Fourier transform of $\hat{F}(t)$ as follows:

$$F(\omega) \equiv \int_{-\infty}^{\infty} \hat{F}(t) e^{-j\omega t}\, dt \tag{32}$$

where ω may be complex.

1) Causal Function: A causal function $\hat{F}(t)$ equals zero for $t < 0$. This implies that $F(\omega)$ is analytic for $\mathrm{Im}(\omega) \leq 0$ and that $\mathrm{Im}(F(\omega)) = \mathcal{H}[\mathrm{Re}(F(\omega))]$, where $\mathcal{H}$ is the Hilbert transform [14], [15].

2) Minimum Phase Function: We call a function $F(\omega)$ minimum phase if both $F(\omega)$ and its reciprocal $1/F(\omega)$ correspond to causal functions in the time domain [15]. Since neither the dependent nor independent variables in the time domain related by a minimum phase function in the frequency domain can occur before the other, *two nonzero signals related by a minimum phase function start simultaneously*.

A minimum phase function is causal; thus, it has the property that its real and imaginary parts are a Hilbert transform pair. In addition, the real and imaginary parts of the complex logarithm of a minimum phase function are a Hilbert transform pair [15]. That is, $\arg(F(\omega)) = \mathcal{H}[\ln |F(\omega)|]$. The minimum phase constraint is much stronger than the causality constraint: it allows the phase of the function to be determined from the Hilbert transform of the logarithm of its magnitude and the magnitude of the function to be determined within a constant multiplier from its phase.

3) Rational Function: A rational function $F(\omega)$ can be written as

$$F(\omega) = \frac{P(\omega)}{Q(\omega)} = \lambda \frac{\prod (\omega - \alpha_i)}{\prod (\omega - \beta_i)} \tag{33}$$

where ω may be complex, λ is a scalar, and $P(\omega)$ and $Q(\omega)$ are polynomials in ω with complex roots α_i and β_i. Except for the multiplier λ, any rational function $F(\omega)$ is entirely described by its zeroes α_i and poles β_i.

4) Pole and Zero Positions: Since causal rational functions are analytic in the lower half of the ω plane defined by $\mathrm{Im}(\omega) < 0$, all of the poles of a causal function $F(\omega)$ must lie in the upper

half of the ω plane [14]. That is, $\mathrm{Im}(\beta_i) > 0$ for all the β_i in (33).

If $F(\omega)$ is minimum phase, then its reciprocal $1/F(\omega)$ is also causal, and its zeroes must also lie in the upper half of the ω plane. That is, both $\mathrm{Im}(\beta_i) > 0$ and $\mathrm{Im}(\alpha_i) > 0$ for all of the α_i and β_i in (33) [15].

Appendix C
Simultaneity of $\boldsymbol{E}_\mathrm{t}$ and $\boldsymbol{H}_\mathrm{t}$

We will now show that $\hat{\boldsymbol{E}}_\mathrm{t}(t, \boldsymbol{r}, 0)$ and $\hat{\boldsymbol{H}}_\mathrm{t}(t, \boldsymbol{r}, 0)$ due to the source in Fig. 1 start simultaneously. Assume that the transverse electric field due to the source has not yet arrived at some transverse coordinate $\boldsymbol{r}$ at the reference plane of Fig. 1 for $t < 0$. That is, we will assume that $\hat{\boldsymbol{E}}_\mathrm{t}(t, \boldsymbol{r}, z) = 0$ for $t < 0$ and $z > 0$. The fields in the region $z > 0$ must satisfy $\nabla \times \hat{\boldsymbol{E}} = -\partial\hat{\boldsymbol{B}}/\partial t$ for $t < 0$, which implies

$$\frac{\partial \hat{\boldsymbol{E}}_\mathrm{z}}{\partial y}\boldsymbol{x} - \frac{\partial \hat{\boldsymbol{E}}_\mathrm{z}}{\partial x}\boldsymbol{y} = -\frac{\partial \hat{\boldsymbol{B}}}{\partial t}. \tag{34}$$

As a result, $\hat{\boldsymbol{B}}_\mathrm{z}(t, \boldsymbol{r}, z) = 0$ for $t < 0$ and $z > 0$.

The fields must also satisfy $\nabla \times \hat{\boldsymbol{H}} = \epsilon\partial\hat{\boldsymbol{E}}/\partial t$ for $t < 0$ and $z > 0$, where ε is the position-dependent permittivity. Since $\hat{\boldsymbol{E}}_t(t, \boldsymbol{r}, z) = \hat{\boldsymbol{B}}_z(t, \boldsymbol{r}, z) = 0$ for $t < 0$ and $z > 0$

$$-\frac{\partial \hat{\boldsymbol{H}}_\mathrm{y}}{\partial z}\boldsymbol{x} + \frac{\partial \hat{\boldsymbol{H}}_\mathrm{x}}{\partial z}\boldsymbol{y} + \left(\frac{\partial \hat{\boldsymbol{H}}_\mathrm{y}}{\partial x} - \frac{\partial \hat{\boldsymbol{H}}_\mathrm{x}}{\partial y}\right)\boldsymbol{z} = \epsilon\frac{\partial \hat{\boldsymbol{E}}_\mathrm{z}}{\partial t}\boldsymbol{z}. \tag{35}$$

This, in turn, implies that

$$\frac{\partial \hat{\boldsymbol{H}}_\mathrm{y}}{\partial z} = \frac{\partial \hat{\boldsymbol{H}}_\mathrm{x}}{\partial z} = 0 \tag{36}$$

for $t < 0$ and $z > 0$. This shows that, except for a dc component, $\hat{\boldsymbol{H}}_\mathrm{t}(t, \boldsymbol{r}, z) = 0$ for $t < 0$ and $z > 0$. Thus, we see that $\hat{\boldsymbol{E}}_\mathrm{t}(t, \boldsymbol{r}, z) = 0$ for $t < 0$ and $z > 0$ implies $\hat{\boldsymbol{H}}_\mathrm{t}(t, \boldsymbol{r}, z) = 0$ there as well, and the transverse magnetic field starts at the reference plane no earlier than the transverse electric field.

A similar argument shows that the transverse electric field starts no earlier than the transverse magnetic field. This completes the argument, showing that neither $\hat{\boldsymbol{E}}_\mathrm{t}(t, \boldsymbol{r}, 0)$ nor $\hat{\boldsymbol{H}}_\mathrm{t}(t, \boldsymbol{r}, 0)$ precedes the other and, thus, that they start simultaneously.

As a consequence, when a guide has a unique wave impedance $Z_\mathrm{w}(\omega)$, both the temporal wave impedance $\hat{\boldsymbol{Z}}_\mathrm{w}(t)$ and the temporal wave admittance $\hat{Y}_\mathrm{w}(t)$ must equal zero for $t < 0$. As a corollary, we see that $Z_\mathrm{w}(\omega)$ and its inverse $Y_\mathrm{w}(\omega) = 1/Z_\mathrm{w}(\omega)$ must be minimum phase.

Appendix D
Error Bound for $|Z_0|$

Assume that we have determined exactly the phase of p_0 up to some frequency ω_0 and that we wish to determine $|Z_0(\omega)|$ at frequencies $\omega < \omega_0$. We will develop an expression bounding the error with which we calculate $|Z_0|$.

The logarithm of $|Z_0|$ is the inverse Hilbert transform of $\arg(p_0)$ as follows:

$$\ln\left|Z_0(\omega)\right| \equiv -\pi^{-1}\int_{-\infty}^{\infty}\frac{\arg\left(p_0(\sigma)\right)}{\sigma - \omega}\,d\sigma. \tag{37}$$

If $b(\omega)$ is the error we make in determining the phase of p_0, we calculate the characteristic impedance Z_0'' from

$$\ln\left|Z_0''(\omega)\right| \equiv -\pi^{-1}\int_{-\infty}^{\infty}\frac{\arg\left(p_0(\sigma)\right) + b(\sigma)}{\sigma - \omega}\,d\sigma. \tag{38}$$

We will always use a condition such as (19) to match the low-frequency limits of $|Z_0|$ and $|Z_0''|$; thus, we can write the magnitude of the characteristic impedance Z_0' we will use in the theory as

$$\left|Z_0'(\omega)\right| = \left|\frac{Z_0(0)}{Z_0''(0)}\right|\left|Z_0''(\omega)\right|. \tag{39}$$

Expanding $\eta(\omega) \equiv \ln|Z_0'| - \ln|Z_0|$ using (37) and (38), we obtain

$$\eta(\omega) = -\omega\pi^{-1}\int_{-\infty}^{\infty}\frac{b(\sigma)}{\sigma(\sigma - \omega)}\,d\sigma. \tag{40}$$

Since $b(\omega)$ is odd and equal to zero for $|\omega| < \omega_0$, we can rewrite (40) as

$$\eta(\omega) = -2\omega^2\pi^{-1}\int_{\omega_0}^{\infty}\frac{b(\sigma)}{\sigma(\sigma^2 - \omega^2)}\,d\sigma. \tag{41}$$

The sign of the real part of p_0 indicates the direction of the real time-averaged power carried by the mode down the guide. If the real part of p_0 for the forward (decaying) mode were negative, the mode would no longer dissipate energy as it propagated down the guide, and violate conservation of energy. Thus, the phase of p_0 can only vary between $\pm\pi/2$, and the error $b(\omega)$ we make in evaluating the phase of p_0 cannot be greater than $\pm\pi$. Since the denominator of (41) is odd, the worst-case error is made when $b(\omega) = \pm\pi$. Thus, we can bound η with

$$\left|\eta(\omega)\right| \le 2\omega^2\int_{\omega_0}^{\infty}\frac{1}{\sigma(\sigma^2 - \omega^2)}\,d\sigma = \ln\frac{\omega_0^2}{|\omega_0^2 - \omega^2|}. \tag{42}$$

Straightforward manipulation gives (21).

Acknowledgment

The authors would like to thank R. C. Wittmann, National Institute of Standards, Boulder, CO, for his many readings of this paper's manuscript in its early stages of preparation and suggesting the approach the authors have presented to reconcile temporal constraints and power normalization.

References

[1] R. B. Marks and D. F. Williams, "A general waveguide circuit theory," *J. Res. Natl. Inst. Stand. Technol.*, vol. 97, no. 5, pp. 533–562, Sept.-Oct. 1992.

[2] N. Marcuvitz, *Waveguide Handbook*, ser. MIT Rad. Lab. New York: McGraw-Hill, 1951, vol. 10.

[3] N. Fache, F. Olyslager, and D. de Zutter, *Electromagnetic and Circuit Modeling of Multiconductor Transmission Lines*. Oxford, U.K.: Clarendon, 1993.
[4] J. R. Brews, "Transmission line models for lossy waveguide interconnections in VLSI," *IEEE Trans. Electron Devices*, vol. ED-33, pp. 1356–1365, Sept. 1986.
[5] R. E. Collins, *Foundations for Microwave Engineering*. New York: McGraw-Hill, 1966.
[6] G. Carrier, M. Krook, and C. Pearson, *Functions of a Complex Variable: Theory and Technique*. New York: McGraw-Hill, 1966.
[7] E. A. Guillemin, *Synthesis of Passive Networks*. New York: Wiley, 1957.
[8] D. F. Williams, "Metal-insulator-silicon transmission line model," in *51st ARFTG Conf. Dig.*, June 12, 1998, pp. 65–71.
[9] D. F. Williams and B. K. Alpert, "Characteristic impedance, power, and causality," *IEEE Microwave Guided Wave Lett.*, vol. 9, pp. 181–182, May 1999.
[10] ——, "Characteristic impedance of microstrip on silicon," in *8th Elect. Performance Electron. Pack. Conf. Dig.*, Oct. 25–27, 1999, pp. 181–184.
[11] D. F. Williams, B. K. Alpert, U. Arz, D. K. Walker, and H. Grabinski, "Causal characteristic impedance of planar transmission lines," *IEEE Trans. Adv. Packag.*, submitted for publication.
[12] F. Olyslager, D. De Zutter, and A. T. de Hoop, "New reciprocal circuit model for lossy waveguide structures based on the orthogonality of the eigenmodes," *IEEE Trans. Microwave Theory Tech.*, vol. 43, pp. 2261–2269, Dec. 1994.
[13] G. Birkhoff and S. Mac Lane, *A Survey of Modern Algebra*. New York: Macmillan, 1965.
[14] C. D. McGillem and G. F. Cooper, *Continuous and Discrete Signal and System Analysis*. New York: Holt, Rinehart, and Winston, 1974.
[15] A. V. Oppenheimer and R. W. Schafer, *Digital Signal Processing*. Englewood Cliffs, NJ: Prentice-Hall, 1975.

Dylan F. Williams (S'82–M'86–SM'90) received the Ph.D. degree in electrical engineering from the University of California at Berkeley, in 1986.

In 1989, he joined the Electromagnetic Fields Division, National Institute of Standards and Technology, Boulder, CO, where he currently develops metrology for the characterization of monolithic microwave integrated circuits and electronic interconnects. He has authored or co-authored over 60 technical papers.

Dr. Williams was the recipient of the Department of Commerce Bronze and Silver Medals, the Electrical Engineering Laboratory's Outstanding Paper Award, two Automatic RF Techniques Group (ARFTG) Best Paper Awards, the ARFTG Automated Measurements Technology Award, and the IEEE Morris E. Leeds Award.

Bradley K. Alpert received the B.S. degree in mathematics from the University of Illinois at Urbana-Champaign, in 1978, the S.M. degree in mathematics from the University of Chicago in 1979, and the Ph.D. degree in computer science from Yale University, New Haven, CT, in 1990.

He was a Casualty Actuary for several years. He was a Hans Lewy Post-Doctoral Fellow at the Lawrence Berkeley Laboratory, University of California at Berkeley. He then joined the National Institute of Standards and Technology, Boulder, CO, in 1991. He was recently a Visiting Researcher at the Courant Institute of Mathematical Sciences, New York University, New York, NY, from 1999 to 2000. His research interests are in scientific computing, including high-order quadratures, wavelets, special functions, and computational electromagnetics.